Solid Freeform Fabrication 2023: Proceedings of the 34th Annual International Solid Freeform Fabrication Symposium – An Additive Manufacturing Conference
Reviewed Paper

Effect of the Print Bed Temperature on Void Distribution within the Microstructure of Short Carbon Fiber Reinforced/ABS Manufactured via Large Area Additive Manufacturing

Neshat Sayah, Dr. Douglas E. Smith,
Department of Mechanical Engineering, Baylor University, Waco, TX, USA

ABSTRACT

Short carbon fiber-reinforced polymer composite structures produced using Large Area Additive Manufacturing (LAAM) have garnered significant attention due to the design flexibility, energy savings, and materials selection associated with this process. However, the physical and mechanical properties of the additively manufactured composite parts often fall below expectations due to void formation between printed beads and within the microstructure of individual beads. This study aims to investigate the effect of bed temperature on the microstructure within the beads of two-layer Short Carbon Fiber reinforced Acrylonitrile Butadiene Styrene (SCF/ABS) beads manufactured via the LAAM system. This study employs high-resolution 3D micro-computed tomography (μCT) to evaluate the void shape and distribution within the microstructure of composite parts printed at various bed temperatures. The results of this study demonstrate substantial variation in the void volume fraction among four bead sets deposited at different print bed temperatures. Moreover, within each part, a noticeable discrepancy in void volume fraction is observed between the top and bottom bead of the two-bead test samples. Preliminary results indicate that increasing the bed temperature from 25°C to 75°C reduces void volume fraction within the microstructure of the composite parts. However, an opposite trend emerges when the bed temperature is further increased to 100°C, increasing void volume fraction, which needs further investigation to understand. This study also evaluated the void shapes through the calculation of their sphericity. The preliminary results reveal that as the bed temperature increases from 25°C to 75°C, the voids exhibit higher sphericity within the printed parts as the interconnected voids decrease.

INTRODUCTION

Polymer composite extrusion-deposition is a widely recognized and favored technique in Additive Manufacturing (AM). This technique stands out among the various AM methods due to the available range of neat thermoplastic polymers and thermoplastic polymer composites that can be utilized [1,2]. Polymer extrusion deposition AM can be implemented in two forms: small scale using Fused Filament Fabrication (FFF) with a liquefier or nozzle filament and large scale employing LAAM with a single screw extruder. This article focuses on the polymer composite extrusion-deposition process via LAAM [3]. Short carbon fibers are used as reinforcements in polymer composites due to improved mechanical and thermal properties compared to neat polymers. However, the properties of the final manufactured polymer composite parts are greatly influenced by their microstructure, which includes factors such as fiber orientation, voids between beads (inter-bead voids), and microstructural voids (intra-bead voids) [4-7]. Insufficient interlayer bonding during polymer composite deposition leads to inter-bead voids forming while intra-bead voids develop within the bead microstructure near the fibers [8-10]. Furthermore, microstructural

voids arise from air entrapment during the manufacturing process and from pre-existing voids present within the filaments or pellets before their utilization in the additive manufacturing process [7,11].

This article specifically centers on microstructural intra-bead voids, which are named 'micro voids' within the body of this article. Optimizing the printing process parameters (i.e., nozzle temperature, bed temperature, nozzle height above the print surface, and extrusion rate) holds substantial potential for enhancing the quality and properties of the final 3D printed polymer composite [12-14]. Most prior research has considered the microstructure of deposited polymer composites employing two-dimensional (2D) imaging techniques, such as electron microscopy. However, the sectional nature of this technique introduces a potential bias when evaluating voids, which can result in errors in the analysis outcomes [15-16]. More recently, researchers have increasingly employed μCT as a viable alternative to avoid potential errors associated with the sectional nature of 2D imaging techniques. μCT offers the advantage of generating high-resolution three-dimensional (3D) structural information for various applications, including the microstructure of additively manufactured polymer composites [17-18]. Despite the previous research on extrusion deposition of polymer composites, there remains to be more information regarding the impact of 3D printing processing parameters on the microstructure of the final manufactured composites, particularly concerning microstructural voids. This study aims to address this gap by presenting an experimental investigation focused on the influence of bed temperature on the void volume fraction, void distribution, and void shape within the microstructure of two-layer SCF/ABS composite beads 3D printed via LAAM, utilizing μCT as the imaging technique.

MATERIALS AND METHODS

3D Printing Process

This research uses the Baylor LAAM system to produce two-layer SCF/ABS polymer composite beads. The Baylor LAAM system appearing in Figure 1 is a custom-built gantry system that incorporates the Strangpresse Model 19 extruder (Strangpresse, Youngstown, OH, USA) [19], which features a single screw extruder with three temperature zones and a nozzle tip diameter of 3.172 mm. For the LAAM feedstock, 13 wt% short carbon fiber (having a diameter of 7.5 microns) PolyOne SCF/ABS pellets (Avient Corporation, Avon Lake, OH, USA) were used. Before starting the 3D printing process, the pellets were dried at 80°C for 12 hours in the oven.

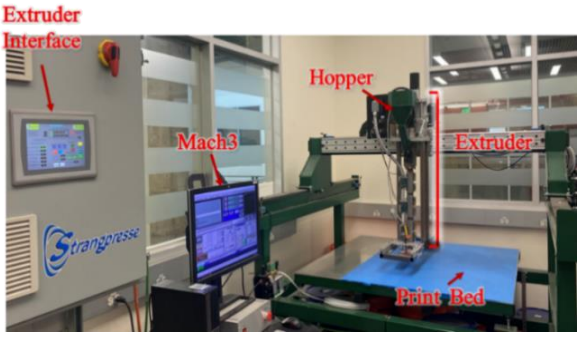

Figure 1. Baylor's custom-built LAAM system [11]

This study used four different bed temperatures (25, 50, 75, and 100 °C) to 3D print two-layer SCF/ABS beads in order to evaluate the effect of bed temperature on their microstructure. It is worth noting that the remaining printing parameters, including the nozzle height above the print bed, nozzle temperature, and extrusion rate, remained unchanged across all printed components. The specific process parameters employed are outlined in Table1.

Nozzle Height	1.1 (mm)
Nozzle Temperature	200 (°C)
Screw Speed	90 (rpm)
Print Speed	101.6 (mm/s)

Table 1. Printing process parameters

µCT Image Acquisition Technique

To acquire accurate and detailed 3D microstructural information of the additively manufactured SCF/ABS parts, the NSI X3000 X-ray µCT system (North Star Imaging, Rogers, MN, USA) was employed in this study. All computed tomography (CT) images were captured at a resolution of 1.7 microns, while the X-ray source was set to generate a voltage of 60kV and a current of 750 µA. Each sample rotated 360 degrees, with increments of 2 degrees, resulting in 1800 projections. The raw data from the µCT system was subsequently imported into efX-CT software (North Star Imaging, Minnesota, USA) for 3D volume reconstruction. The reconstructed data was then imported into VGStudio Max 3.4 software (Volume Graphics GmbH, Heidelberg, Germany) for void analysis. The VGDefX algorithm was employed for void evaluation, which used grayscale data at the voxel scale to detect and analyze voids within the microstructure of each scanned part [11,20].

RESULTS AND DISCUSSIONS

As discussed earlier in Section 2 of this study, µCT offers comprehensive microstructural details of the scanned parts. Figure 2 shows a 2D cross-section sample from a SCF/ABS bead printed on a bed with a temperature of 100°C which highlights the observed microstructural, including micro voids, short carbon fibers, and the polymer matrix.

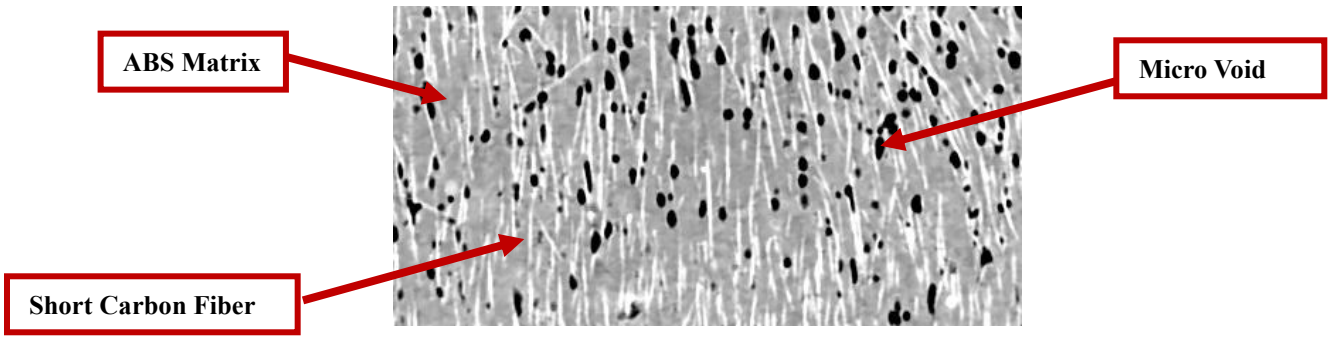

Figure 2. Microstructural features of SCF/ABS part printed on a bed with a temperature of 100°C

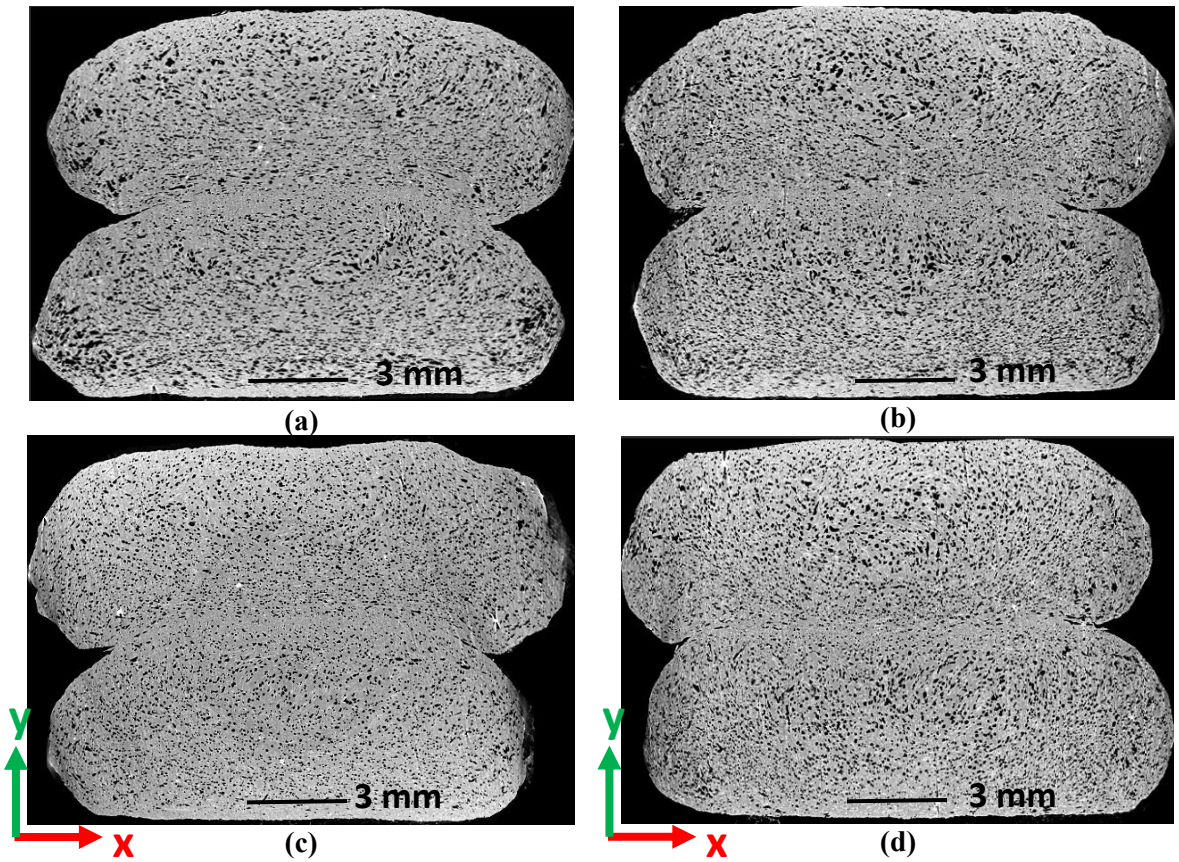

Figure 3. 2D cross-sections obtained from µCT scans of the two-layer SCF/ABS beads manufactured on beds with different temperatures: a) print bed temperature of 25°C, b) print bed temperature of 50°C, c) print bed temperature of 75°C, and d) print bed temperature of 100°C.

Figure 3 presents the 2D cross-sections of the four scanned two-layer SCF/ABS beads that were printed for this study. The printing parameters remained consistent across all samples, except for the bed temperature variation for each additively manufactured part, as explained in Table 1. The µCT images reveal variations in the bead's shape, void content, and void shape within the microstructure of each two-layer bead. Also shown is a significant variation in microstructure over the cross-section of the bead. A significant presence of micro voids is evident within the bottom and top beads printed on a print bed temperature of 25°C, as shown in Figure 3(a). Furthermore, notable occurrences of large micro voids and interconnected voids are particularly prominent along the edges and near the print bed area. Figure 3(b) shows the microstructure of the two-layer bead printed on a print bed with a temperature of 50°C, revealing a significant number of micro voids. However, compared to the two-layer beads printed on a print bed temperature of 25°C (Figure 3(a)), the quantity of large micro voids and interconnected voids is reduced, particularly near the print bed area and the edges. However, it is essential to note that there is still evidence of large and interconnected voids near the center of both the top and bottom beads, as highlighted in Figure 3(b). Figure 3(c) illustrates that the quantity of voids within the microstructure of the two-layer beads printed on a print bed with a temperature of 75°C has significantly decreased compared to those printed on print beds at 25°C and 50°C. Furthermore, micro voids appearing in Figure 3(c) are notably smaller, with very few large micro voids in both the top and bottom bead

microstructures. In the microstructure of the two-layer beads 3D printed on a print bed with a temperature of 100°C, a notable presence of voids is observed in both the top and bottom beads, as shown in Figure 3(d). The void content is relatively lower than in the bead printed on a print bed with a temperature of 75°C. However, the micro void content and the presence of large and interconnected voids are lower in comparison to the 25°C and 50°C print bed samples.

To investigate the influence of bed temperature on micro voids within the bead microstructure, an analysis was performed on the void volume fraction present in both the top and bottom beads of each 3D-printed two-layer composite. The measured results appear in Table 2, indicating that the void volume fraction exhibits variations within the microstructure of the two-layer beads printed at different bed temperatures and within each part's top and bottom beads. Furthermore, for a more comprehensive understanding of the micro void distribution within the microstructure of each bead, an evaluation of the void volume fraction was conducted along the coordinate direction of each bead. The results are presented in Figures (4-6). It is worth noting that the Z-direction corresponds to the extrusion (print) direction, while the Y-direction is perpendicular to the print surface for all parts.

Bed Temperature (°C)	Bottom bead average void volume fraction (%)	Top bead average void volume fraction (%)
25	12.86	12.08
50	12.25	11.87
75	8.74	9.15
100	10.89	11.23

Table 2. Average void volume fraction within the top and bottom beads of two-layer SCF/ABS printed on various bed temperatures

Figure 4(a) illustrates the void volume fraction distribution within the microstructure of the SCF/ABS composite. In both the top and bottom beads printed on a bed with a temperature of 25°C, a higher void volume fraction is observed along the edges, gradually decreasing toward the center of the beads. Along the X-coordinate direction, the bottom bead consistently exhibits a higher void volume fraction than the top. Figure 4(b) presents the void volume fraction distribution within the microstructure of the two-layer bead printed on a bed temperature of 50°C. Like the bottom bead on the bed temperature of 25°C, a higher void volume fraction is observed along the edges of the bottom bead, which gradually decreases towards the bead center. In contrast, the top bead exhibits the opposite behavior, with a higher void volume fraction at the center and lower along the edges. Figure 4(c) illustrates the void volume fraction variation along the X-coordinate direction of the two-layer bead printed on a bed temperature of 75°C. Compared to the part printed on bed temperatures of 25°C and 50°C, a significant reduction in void volume fraction is observed in both the top and bottom beads. This observation indicates that increasing the bed temperature from 25°C to 75°C decreases the void volume fraction within the 3D printed part. Figure 4(d) demonstrates the void volume fraction along the X-coordinate direction of the part printed on a bed temperature of 100°C. It can be observed that the void volume fraction with a 100°C print bed is higher compared to the part printed on a bed temperature of 75°C but lower than those printed on bed temperatures of 25°C and 50°C. Additionally, within the top bead, the void volume fraction is higher near the center of the bead, while it is lower in the bottom bead. The findings in Figure 4

highlight the variation in void volume fraction within different regions of the composite part, depending on the bed temperature during printing. Furthermore, the micro void distribution behavior within the top and bottom beads of each two-layer SCF/ABS composite exhibits inhomogeneous spatial patterns.

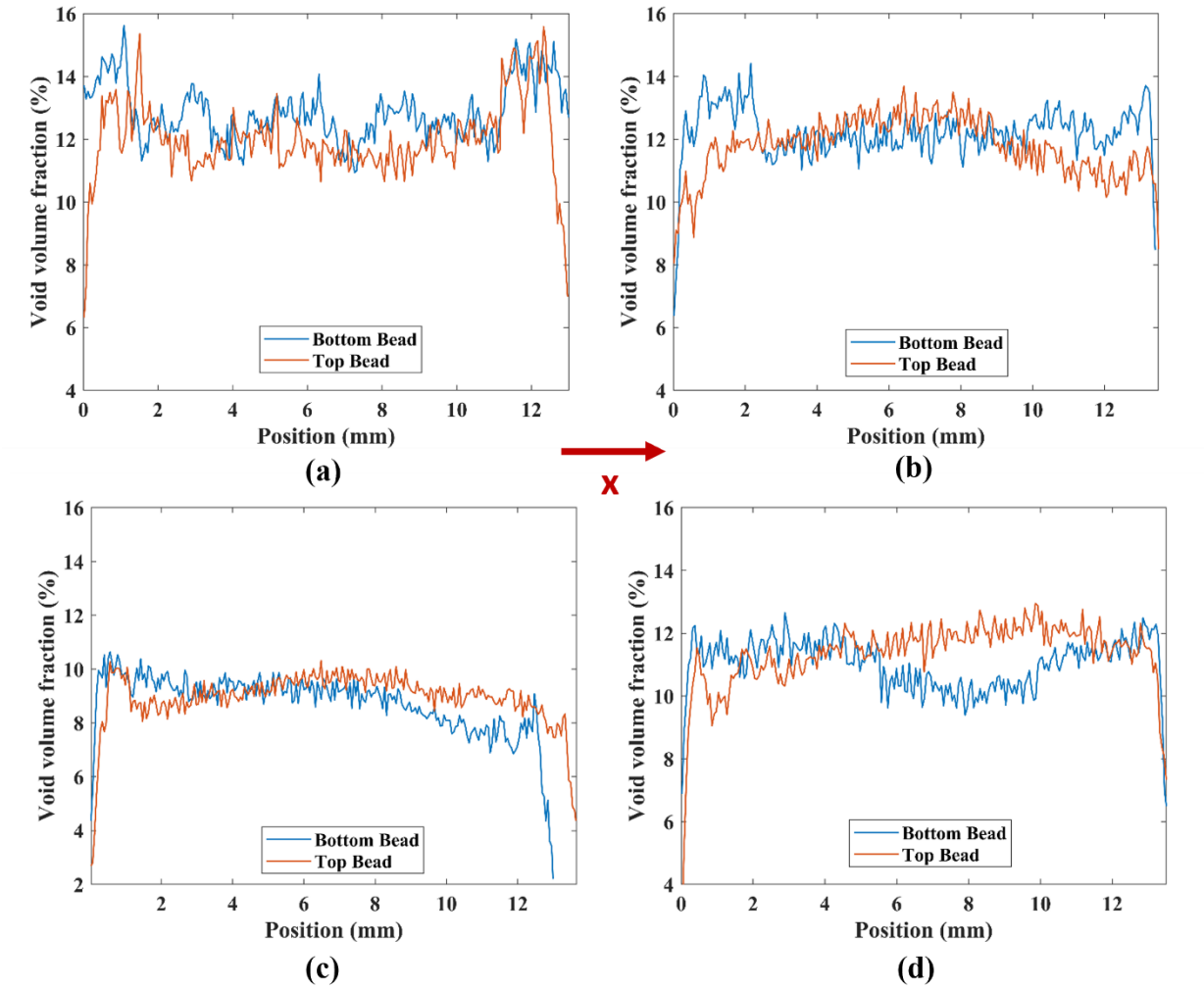

Figure 4. Void volume fraction along the X-coordinate direction of two-layer SCF/ABS beads printed on beds with different temperatures: a) print bed temperature of 25°C, b) print bed temperature of 50°C, c) print bed temperature of 75°C, and d) print bed temperature of 100°C.

Figure 5 presents the void volume fraction along the Y-coordinate direction (normal to the print surface) of the beads printed at different bed temperatures. Across all bottom beads, a lower void volume fraction is observed near the print bed, which gradually increases towards the center of the bead. Notably, a significant increase in void volume fraction is detected just before the interface with the top bead, followed by a notable reduction at the interface itself. A comparative analysis of the void volume fraction within the microstructure of the top beads, printed at different bed temperatures, reveals distinct patterns. In all top beads, the void volume fraction is notably low, close to the interface between the top and bottom beads. However, the volume fraction gradually

increases, moving toward the center of the top beads. The void volume fraction is also consistently low near the surface across all additively manufactured parts.

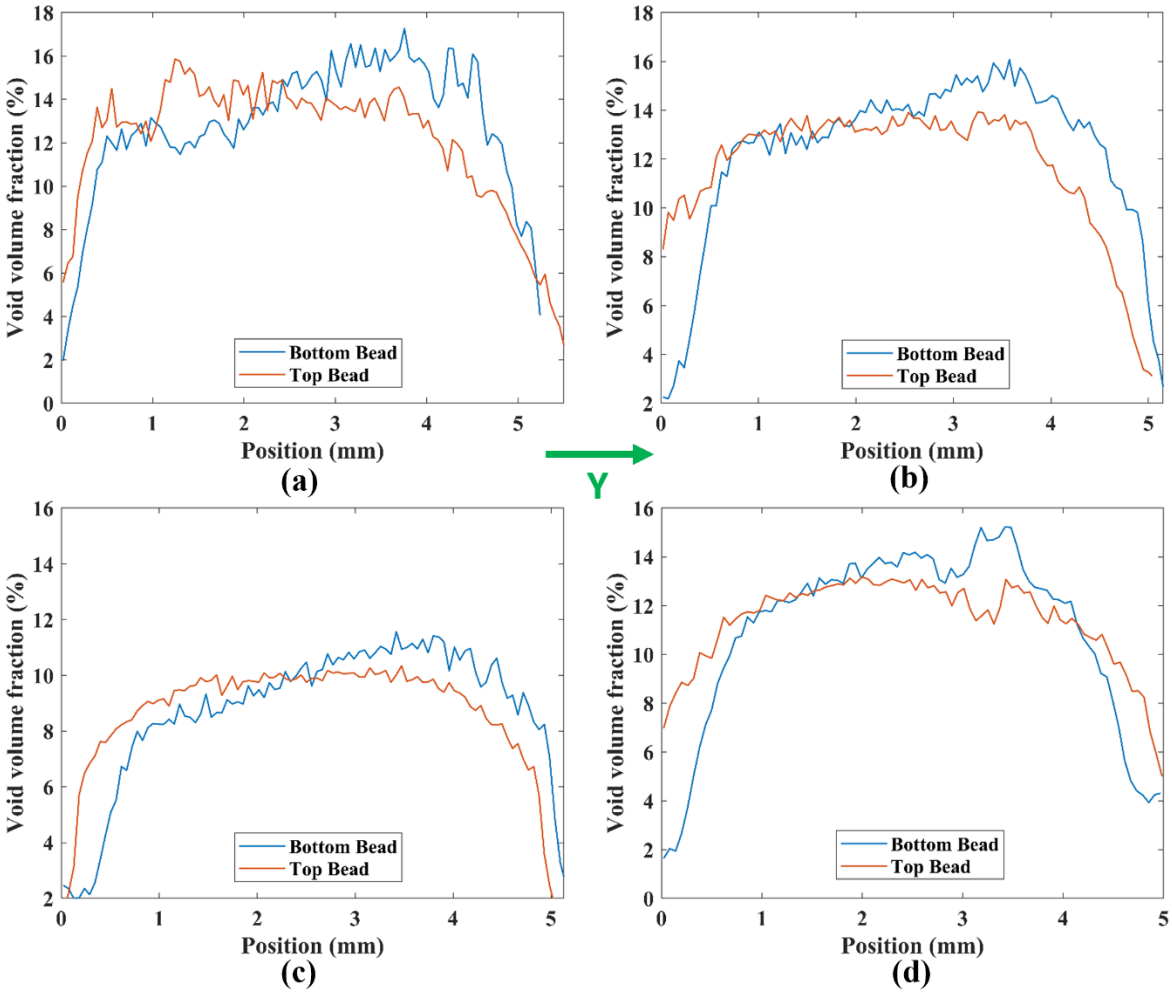

Figure 5. Void volume fraction along the Y-coordinate direction of two-layer SCF/ABS beads printed on beds with different temperatures: a) print bed temperature of 25°C, b) print bed temperature of 50°C, c) print bed temperature of 75°C, and d) print bed temperature of 100°C.

Figure 6 shows the volume fraction variation along the Z coordinate direction (corresponding to the 3D print direction) in two-layer SCF/ABS composites printed at different bed temperatures. Results indicate that unlike the variations observed along the X and Y-coordinate directions, the void volume fraction remains relatively constant along the print direction in both the top and bottom beads, as expected. Furthermore, this analysis reveals that the distribution of micro voids differs depending on the bed temperature. Specifically, in parts printed at bed temperatures of 25°C and 50°C, the void volume fraction is higher within the bottom beads. In contrast, the void volume fraction is higher within the top beads in parts produced at bed temperatures of 75°C and 100°C.

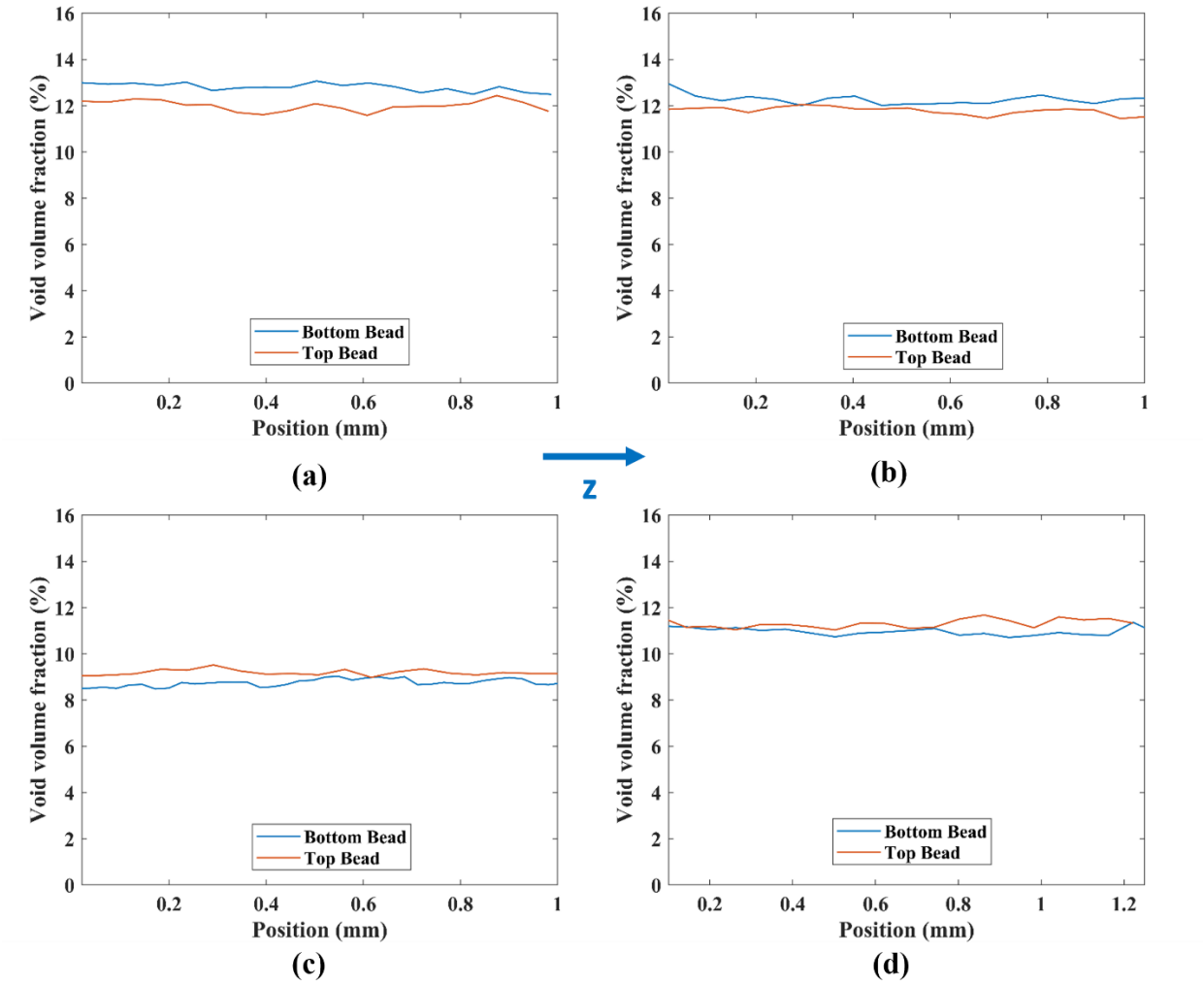

Figure 6. Void volume fraction along the Z-coordinate direction of two-layer SCF/ABS beads printed on beds with different temperatures: a) print bed temperature of 25°C, b) print bed temperature of 50°C, c) print bed temperature of 75°C, and d) print bed temperature of 100°C.

The microstructure of each void within the two-layer SCF/ABS composites was subjected to further analysis to obtain detailed insights into their shapes. Void sphericity, which is determined by comparing the surface area of the detected void with the surface area of a sphere with the same volume as the void, was employed to evaluate the shape characteristics of the micro voids. Note that a void with a perfectly spherical shape has a sphericity value of 1, while sphericity decreases as voids assume more irregular shapes. To ensure accurate results, voids of less than five voxels were excluded from the sphericity calculations, mitigating the impact of voxel size on the obtained sphericity values. A two-parameter Weibull distribution, given as:

$$f(x) = (b/a)(x/a)^{(b-1)}(e)^{-(\frac{x}{a})^b} \qquad x \geq 0 \qquad (1)$$

was used to model the void sphericity distribution with parameters a and b representing the scale and shape parameters, respectively, which are presented in Table 3. Figure 7 displays a histogram

of the measured data, accompanied by a fitted Weibull curve that depicts the fraction of voids across the measured sphericity range for all four SCF/ABS 3D printed parts.

Bed Temperature (°C)	Weibull distribution scale parameter (a)	Weibull distribution shape parameter (b)
25	0.56	7.64
50	0.58	8.02
75	0.63	8.92
100	0.60	8.21

Table 3. Weibull distribution parameters on void sphericity of two-layer SCF/ABS beads printed on beds with different temperatures

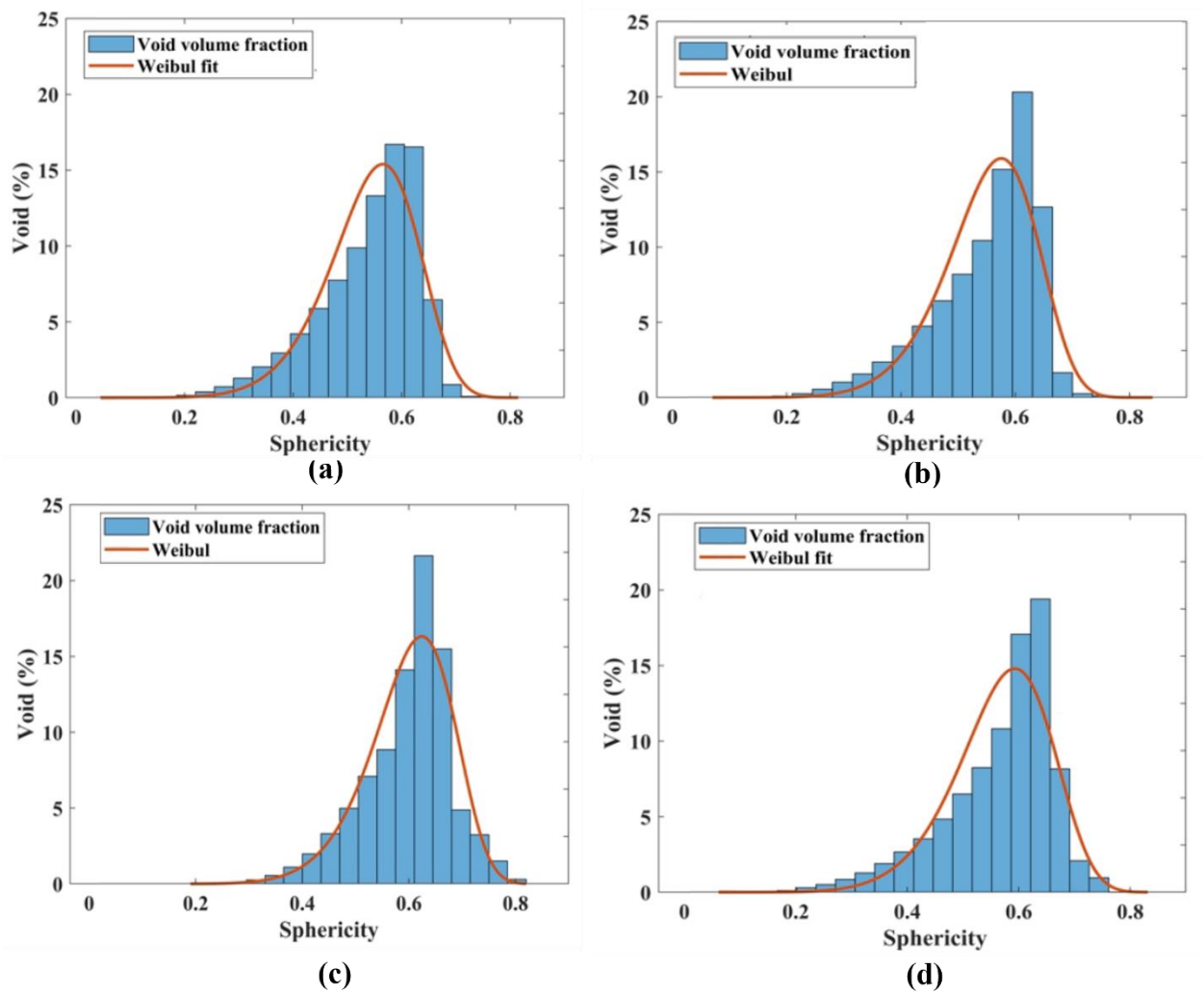

Figure 7. Void sphericity and Weibull fit of two-layer SCF/ABS beads printed on beds with different temperatures: a) print bed temperature of 25°C, b) print bed temperature of 50°C, c) print bed temperature of 75°C, and d) print bed temperature of 100°C

Figures 7(a) and 7(b) demonstrate the distribution of void sphericity in relation to the SCF/ABS part printed on bed temperatures of 25°C and 50°C, respectively. These figures reveal a considerable presence of voids with sphericity values below 0.5 (indicating irregular-shaped voids). In contrast, a smaller portion of voids exhibits sphericity values above 0.70 (indicative of more spherical-shaped voids). Furthermore, Figure 7(c) reveals that, among the four additively manufactured two-layer SCF/ABS parts, the sample printed on the bed with a temperature of 75°C exhibits a greater abundance of voids with higher sphericity values, indicating a more spherical shape. Specifically, a significant portion of the voids in this sample display sphericity values above 0.70. However, it is worth noting that voids within the sphericity range of 0.31-0.5 are still present in this particular sample. Figure 7(d) demonstrates that the void sphericity distribution within the composite printed on a bed temperature of 100°C resembles those printed on beds with 25°C and 50°C. The main distinction lies in the higher number of voids exhibiting a sphericity value greater than 0.7 in the sample produced at 100°C. µCT images also reveal distinctive microstructural characteristics at the interface between the top and bottom beads within the SCF/ABS-additively manufactured composites.

Figure 8 provides 2D µCT images showing microstructural features at the interfaces of the printed parts.

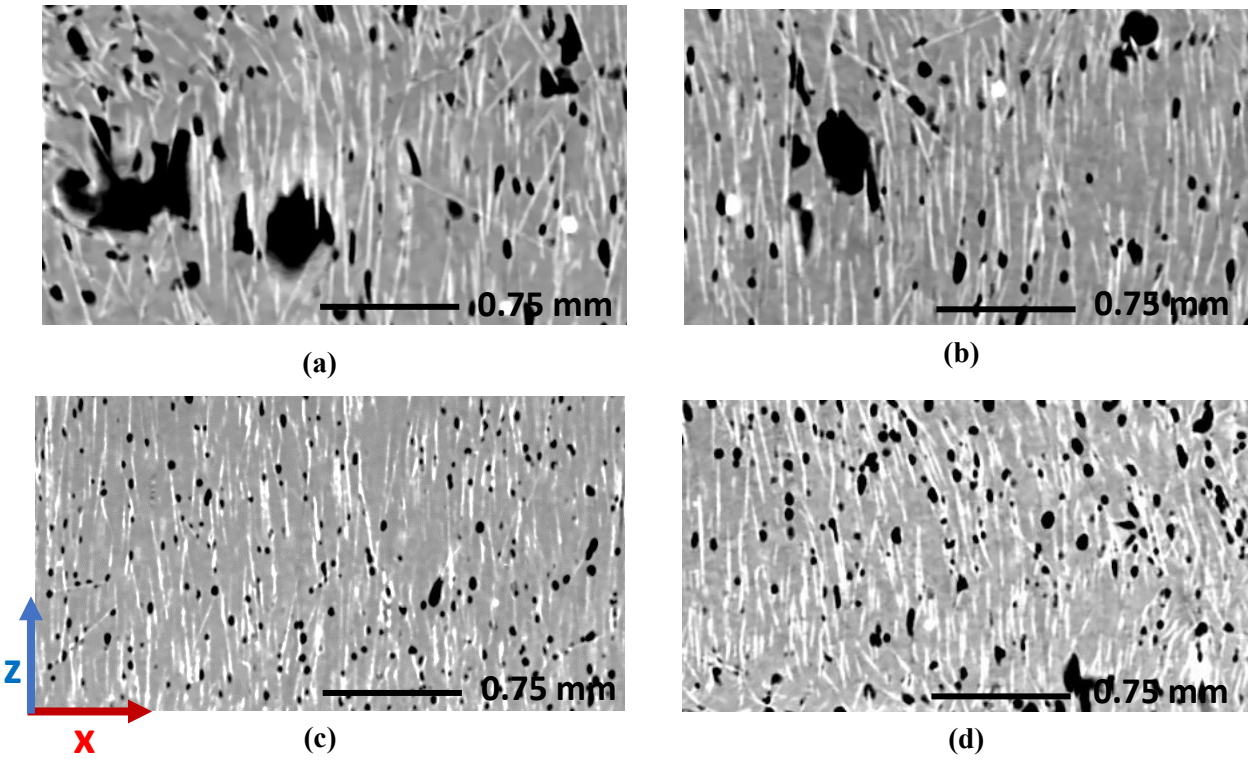

Figure 8. 2D µCT image of the microstructural features at the interface of two-layer SCF/ABS beads printed on beds with different temperatures: a) print bed temperature of 25°C, b) print bed temperature of 50°C, c) print bed temperature of 75°C, and d) print bed temperature of 100°C.

Figure 8(a) shows that at the interface of the part printed on a print bed with a temperature of 25°C, elongated voids, larger voids, and interconnected voids are observed alongside smaller voids. Figure 8(b) shows that the number of voids is reduced in the part printed on a bed with a temperature of 50°C. Although a few large voids and some interconnected voids are present, their occurrence is less frequent compared to the part printed at 25°C. No significant presence of large or interconnected voids is detected at the interface of the two-layer composite printed on the bed with a temperature of 75°C (Figure 8(c)). The voids observed in this case are considerably smaller and exhibit a more spherical shape than those in parts printed at 25°C and 50°C. Furthermore, Figure 8(d) highlights the presence of small voids, with only a few interconnected voids, at the interface of the two-layer composite 3D printed on a bed with a temperature of 100°C. This indicates that increasing the bed temperature from 25°C to 75°C causes a significant reduction in the average void volume fraction within the microstructure of the additively manufactured SCF/ABS composite and the number of interconnected voids at the interface. It is worth mentioning that although the void sizes are larger at the interface of the part printed on a bed temperature of 100°C compared to the one printed on a bed with a temperature of 75°C, they are smaller with a significantly lower number of interconnected voids compared to those printed at bed temperatures of 25°C and 50°C.

CONCLUSION

This study aims to evaluate the influence of bed temperature on various aspects of the microstructure of two-layer SCF/ABS composites 3D printed with the Baylor LAAM system, employing μCT as the analysis technique. To achieve this, four composite parts were printed using identical printing process parameters but varying bed temperatures of 25°C, 50°C, 75°C, and 100°C. The void volume fraction within the microstructure of these additively manufactured composites was subsequently measured. The results show significant differences in the void volume fraction among the four printed parts. Furthermore, within each part, there was variation in void volume fraction between the top and bottom bead regions. Increasing the bed temperature from 25°C to 50°C reduced the void volume fraction from 12.47% to 12.06%, corresponding to a 5.33% decrease. Additionally, raising the bed temperature from 50°C to 75°C led to a substantial reduction in void volume fraction of 25.78% (from 12.06% to 8.95%). However, increasing the bed temperature from 75°C to 100°C caused an increase in void volume fraction from 8.95% to 11.11%, which warrants further investigation better to understand the underlying behavior and cause of this increase. This study also conducted a comprehensive analysis of void shapes by calculating their sphericity. The findings revealed that increasing the bed temperature from 25°C to 75°C resulted in higher sphericity of voids, indicating a more spherical shape within the printed beads. This temperature increase was also associated with a reduced presence of interconnected voids. Conversely, as observed in the void volume fraction trends, raising the bed temperature from 75°C to 100°C decreased void sphericity. The microstructural characteristics, including void shape, were further examined at the interfaces of each printed composite part. The findings revealed that increasing the bed temperature from 25°C to 75°C substantially reduced the presence of interconnected voids. This reduction led to smaller void and a more spherical shape of the voids. At a bed temperature of 100°C, the voids were significantly smaller, and only a few interconnected voids were observed compared to those printed at 25°C and 50°C. However, it is worth noting that

the voids at the interface of the part printed at 100°C were larger than those at 75°C. These observations highlight the intricate relationship between bed temperature and void characteristics, indicating that higher temperatures contribute to forming smaller, more spherical voids with fewer interconnected voids.

ACKNOWLEDGMENT

The authors would like to express their gratitude to the US National Science Foundation (grant #2055628) for their financial support and to Strangpresse for providing the Model 19 extruder used in this study.

REFERENCES

[1] T. Mulholl, S. Goris, J. Boxleitner, T.A. Osswald, and N. Rudolph, "Process-induced fiber orientation in fused filament fabrication". Journal of Composites Science, 2(3), p.45, 2018.

[2] K.M.M. Billah, F.A. Lorenzana, N.L. Martinez, R.B. Wicker and D.Espalin. "Thermomechanical characterization of short carbon fiber and short glass fiber-reinforced ABS used in large format additive manufacturing". Additive Manufacturing, 35, p.101299, 2020.6

[3] Pibulchinda, P., Barocio, E., Favaloro, A.J. and Pipes, R.B., 2023. Influence of printing conditions on the extrudate shape and fiber orientation in extrusion deposition additive manufacturing. *Composites Part B: Engineering*, *261*, p.110793.

[4] Yu, S., Bale, H., Park, S., Hwang, J.Y. and Hong, S.H., 2021. Anisotropic microstructure dependent mechanical behavior of 3D-printed basalt fiber-reinforced thermoplastic composites. Composites Part B: Engineering, 224, p.109184.

[5] D. Yang, H. Zhang, J. Wu, and E.D. McCarthy. "Fibre flow and void formation in 3D printing of short fibre reinforced thermoplastic composites: an experimental mark exercise". Additive Manufacturing, 37, p.101686, 2021.

[6] H.L. Tekinalp, V. Kunc, G.M. Velez-Garcia, C.E. Duty, L.J. Love., A.K. Naskar, , C.A. Blue,and S. Ozcan. "Highly oriented carbon fiber–polymer composites via additive manufacturing". Composites Science and Technology, 105, pp.144-150, 2014.

[7] Sosa-Rey, F., Abderrafai, Y., Lewis, A.D., Therriault, D., Piccirelli, N. and Lévesque, M., 2022. OpenFiberSeg: Open-source segmentation of individual fibers and porosity in tomographic scans of additively manufactured short fiber reinforced composites. Composites Science and Technology, 226, p.109497.

[8] Wang, Z., Fang, Z., Xie, Z. and Smith, D.E., 2022. A Review on Microstructural Formations of Discontinuous Fiber-Reinforced Polymer Composites Prepared via Material Extrusion Additive Manufacturing: Fiber Orientation, Fiber Attrition, and Micro-Voids Distribution. Polymers, 14(22), p.4941.

[9] Awenlimobor, A., Smith, D.E., Wang, Z. and Luo, C., 2022. Three-dimensional (3D) Simulation of Micro-Void Development within Large Scale Polymer Composite Deposition Beads. In 2022 International Solid Freeform Fabrication Symposium.

[10] Awenlimobor, A., Wang, Z. and Smith, D.E., 2021. Physical Modeling: Simulation of Micro-Void Development within Large Scale Polymer Composite Deposition Beads. In 2021 International Solid Freeform Fabrication Symposium. University of Texas at Austin.

[11] Sayah, N. and Smith, D.E., 2022. Effect of Process Parameters on Void Distribution, Volume Fraction, and Sphericity within the Bead Microstructure of Large-Area Additive Manufacturing Polymer Composites. Polymers, 14(23), p.5107.

[12] Wright, W.J., Koerner, H., Rapking, D., Abbott, A. and Celik, E., 2022. Rapid fiber alignment quantification in direct write printing of short fiber reinforced composites. *Composites Part B: Engineering*, *236*, p.109814.

[13] Yu, S., Bale, H., Park, S., Hwang, J.Y. and Hong, S.H., 2021. Anisotropic microstructure dependent mechanical behavior of 3D-printed basalt fiber-reinforced thermoplastic composites. *Composites Part B: Engineering*, *224*, p.109184.

[14] Hmeidat, N.S., Elkins, D.S., Peter, H.R., Kumar, V. and Compton, B.G., 2021. Processing and mechanical characterization of short carbon fiber-reinforced epoxy composites for material extrusion additive manufacturing. *Composites Part B: Engineering*, *223*, p.109122.

[15] Sommacal, S., Matschinski, A., Drechsler, K. and Compston, P., 2021. Characterisation of void and fiber distribution in 3D printed carbon-fiber/PEEK using X-ray computed tomography. Composites Part A: Applied Science and Manufacturing, 149, p.106487.

[16] Garcea, S.C., Wang, Y. and Withers, P.J., 2018. X-ray computed tomography of polymer composites. Composites Science and Technology, 156, pp.305-319.

[17] Diouf-Lewis, A., Farahani, R.D., Iervolino, F., Pierre, J., Abderrafai, Y., Lévesque, M., Piccirelli, N. and Therriault, D., 2022. Design and characterization of carbon fiber-reinforced PEEK/PEI blends for Fused Filament Fabrication additive manufacturing. Materials Today Communications, 31, p.103445.

[18] Dana, H.R., Barbe, F., Delbreilh, L., Azzouna, M.B., Guillet, A. and Breteau, T., 2019. Polymer additive manufacturing of ABS structure: Influence of printing direction on mechanical properties. Journal of Manufacturing Processes, 44, pp.288-298.

[19] https://strangpresse.com

[20] Wang, X., Zhao, L., Fuh, J.Y.H. and Lee, H.P., 2019. Effect of porosity on mechanical properties of 3D printed polymers: Experiments and micromechanical modeling based on X-ray computed tomography analysis. Polymers, 11(7), p.1154.